ELSEVIER

Journal of Alloys and Compounds 417 (2006) 180–186

Journal of ALLOYS AND COMPOUNDS

www.elsevier.com/locate/jallcom

Interfacial reaction and shear strength of Pb-free SnAg2.5Cu0.8Sb0.5 and SnAg3.0Cu0.5Sb0.2 solder bumps on Au/Ni(P) metallization

Ying-Chao Hsu [a], Yuan-Ming Huang [a], Chih Chen [a,*], Henry Wang [b]

[a] *Department of Materials Science and Engineering, National Chiao Tung University, Hsin-chu 300, Taiwan, ROC*
[b] *Accurus Scientific Co., Ltd, Tainan County, Taiwan, ROC*

Received 28 March 2005; accepted 28 June 2005
Available online 9 December 2005

Abstract

This study investigates the metallurgical reaction and shear strength of Pb-free SnAg2.5Cu0.8Sb0.5 and SnAg3.0Cu0.5Sb0.2 solder bumps on Au/Ni(P) metallization pads. It is found that $(Cu,Ni)_6Sn_5$ intermetallic compound (IMC) formed at the interface between the Sn2.5Ag0.8Cu0.5Sb solder and the metallization pad; whereas $(Cu,Ni)_6Sn_5$ and $(Ni,Cu)_3Sn_4$ IMCs formed when the SnAg3.0Cu0.5Sb0.2 reacted with the Au/Ni(P) metallization pad. The difference in the Cu concentration in the two solders may be responsible for the different interfacial IMC formation. The shear strengths for the SnAg2.5Cu0.8Sb0.5, SnAg3.0Cu0.5Sb0.2, SnAg3.0Cu0.5, and SnAg4.0Cu0.5 solders were also measured. The shear strength test revealed that the SnAg2.5Cu0.8Sb0.5 solder has the highest shear strength, which may be due to the solid-solution strengthening of the Sb atoms.

Keyword: Intermetallics

1. Introduction

With the increase of environmental concerns, the use of Pb-free solders for consumer electronic products has become a market driving force [1,2]. For example; the Congress of the European Union has decided to ban the use of Pb-based solders from 1 July 2006. Among the Pb-free solders, eutectic SnAg3.8Cu0.7 solder appears to be the most promising candidate for replacing the eutectic SnPb solder. Moreover, the National Electronics Manufacturing Initiative (NEMI) has recommended replacing the eutectic SnPb solder with the eutectic SnAgCu alloy in reflow processing [3]. The eutectic SnAgCu solder has excellent mechanical properties and electromigration resistance compared with the eutectic SnPb solder [4], nevertheless, the fast consumption of under-bump metallization (UBM), which results in the spalling of intermetallic compound (IMC) into the solder, is a challenging issue for the SnAgCu solder [5].

Several researchers have reported that the addition of Sb and other solid solution atoms (Ge, for example) retard the growth of intermetallic compounds and also improve the mechanical property its of the SnAg solder [6–9]. Ma et al. reported that the SnAg2Cu0.8Sb0.6 solder exhibited a slower Cu–Sn IMC growth rate than the SnAg3.8Cu0.7 solder [7]. Chen et al. examined the influence of Sb on the IMC growth in the SnAgCuSb solder on a Cu substrate during reflow process [8]. They found that both the thickness and the grain size of the Cu_6Sn_5 IMC decreased when the Sb was added. Lee et al. investigated the effect of the Sb addition on the adhesive strength of Cu/Sn–Ag/Cu solder wires, finding that the SnAg solder with 1.5% Sb had the best adhesive strength [9]. Amagai et al. investigated the effect of additives on drop test performance of SnAg2.3 based solder, finding that the addition of Sb can improve the performance drop test performance [6], Therefore, the addition of Sb into the SnAgCu solder is feasible and it has potential application in Pb-free solder joints.

Two commercially-available solders containing Sb are SnAg2.5Cu0.8Sb0.5 and SnAg3.0Cu0.5Sb0.2, which are also known as Castin I and Castin II. However, the interfacial reaction of SnAg2.5Cu0.8Sb0.5 and SnAg3.0Cu0.5Sb0.2 on the Au/Ni(P) metallization pad has not been studied. In addition, the effect of adding Sb on shear strength of the SnAgCu solder has also not been investigated. This paper investi-

* Corresponding author.
E-mail address: chih@cc.nctu.edu.tw (C. Chen).

0925-8388/$ – see front matter © 2005 Elsevier B.V. All rights reserved.
doi:10.1016/j.jallcom.2005.06.087

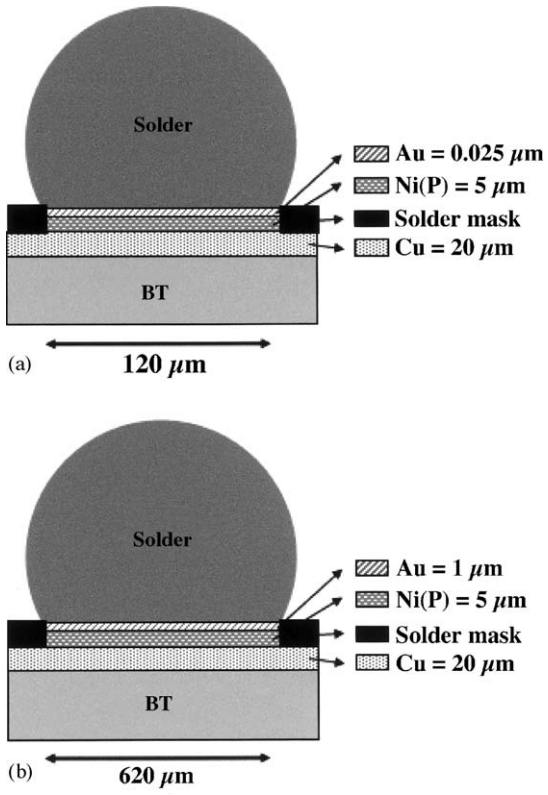

Fig. 1. Schematic illustration of the two sets of samples used in this study: (a) sample for interfacial reaction and (b) test sample for shear strength.

gates the interfacial reaction of the SnAg2.5Cu0.8Sb0.5 and the SnAg3.0Cu0.5Sb0.2 solders on the Au/Ni(P) metallization pad. In addition, we also performed shear tests for the SnAg2.5Cu0.8Sb0.5, SnAg3.0Cu0.5Sb0.2, SnAg3.0Cu0.5, and SnAg4.0Cu0.5 solder bumps. This research provides a further understanding of interfacial reaction and the shear strength of SnAgCuSb solders on Au/Ni(P) metallization pad.

2. Experimental

The experimental procedure is divided into two parts, as described below. The first part focused on the interfacial reaction of the SnAg2.5Cu0.8Sb0.5 and SnAg3.0Cu0.5Sb0.2 solders with the Au/Ni(P) pad metallization on a bismaleimide triazine (BT) substrate. The above sets of samples are illustrated schematically in Fig. 1(a). The pad metallization consisted of 0.025 μm Au/5 μm Ni(P), in which the Ni(P) layer was electroless-plated on the BT substrate side with the diameter of the metallization opening at 144 μm. The solders were pre-heated at 150 °C for 1 min, and then were reflowed at 250 °C on the Au/Ni(P) pad for 1, 5, 10, and 20 min on a hotplate. The samples were observed from both cross-sectional and plan views. Cross-sectional samples were prepared by grinding and polishing laterally to the approximate center of the bumps for microstructure examination. The plan-view samples were prepared by grinding from the top to the middle of the solder bumps, and they were then selectively etched by a solution of HNO_3:CH_3COOH:$C_3H_5(OH)_3$ at the ratio of 1:1:1 in order to etch away Sn.

The second part in this research is to investigate the shear strength of SnAg2.5Cu0.8Sb0.5, SnAg3.0Cu0.5Sb0.2, SnAg3.0Cu0.5 and SnAg4.0Cu0.5 solder bumps. Twenty solder bumps were prepared in each die by pick-n-place of 760 μm solder balls on BT substrates, with a metallization layer consisting of 1 μm Au and 5 μm electroless Ni(P), and with a 620 μm diameter of the metallization opening. The schematic diagram of the test sample is illustrated in Fig. 1(b). The solders were pre-heated at 150 °C for 1 min then reflowed at 250 °C for 1 min. After the reflow process, some of samples were placed in a furnace in the atmosphere for high temperature storage at 150 °C for 1000 h.

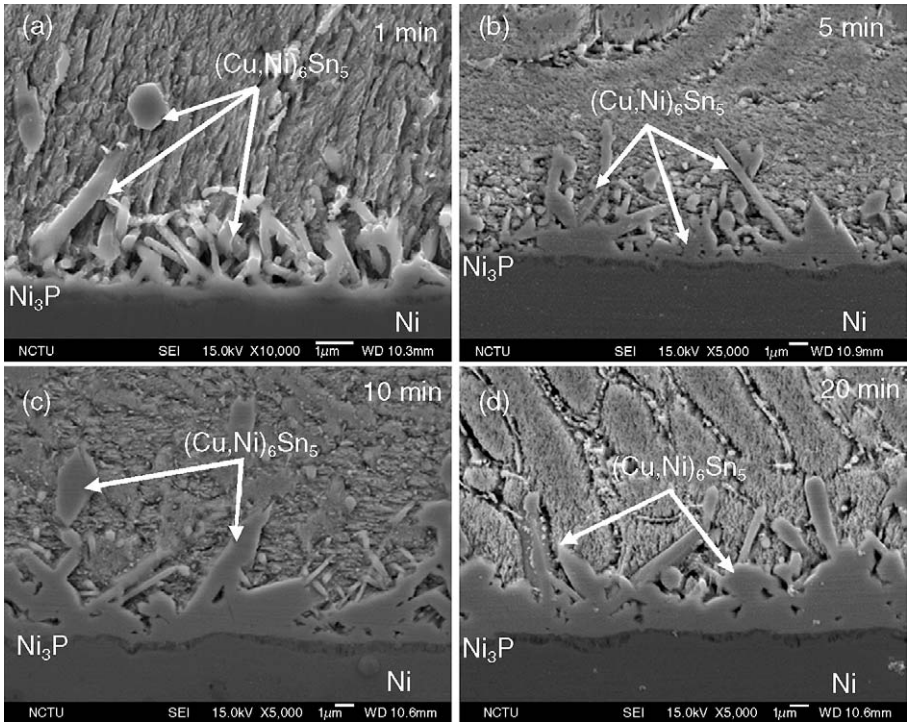

Fig. 2. Cross-sectional SEM images of the interfacial microstructure between the SnAg2.5Cu0.8Sb0.5 solder and the Au/Ni(P) metallization after reflow for (a) 1 min, (b) 5 min, (c) 10 min, and (d) 20 min. Intermetallic compound of $(Cu,Ni)_6Sn_5$ formed at the interface.

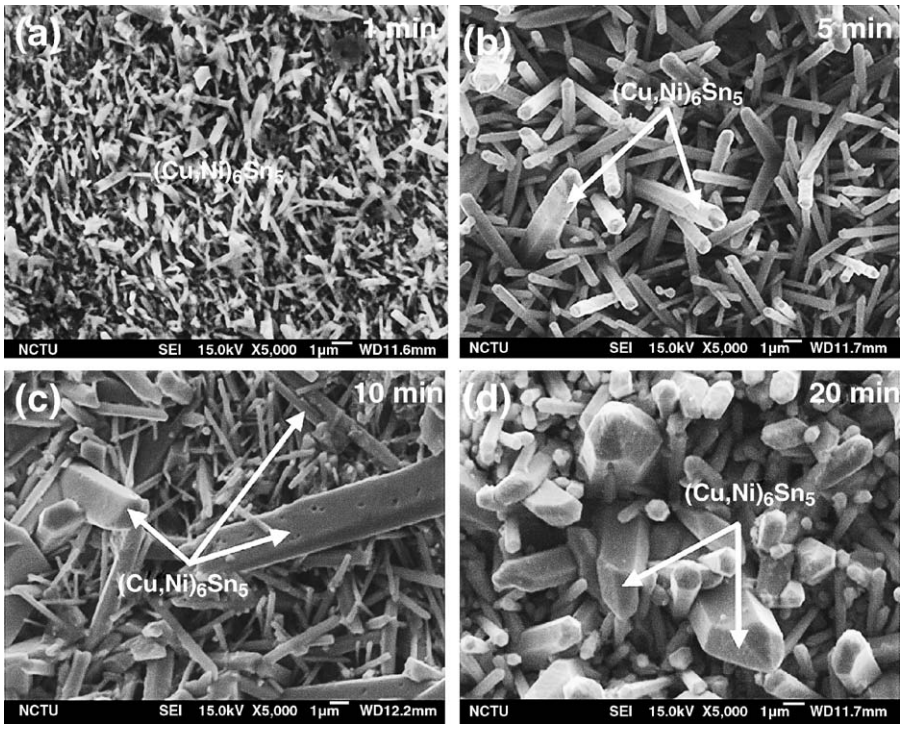

Fig. 3. Plan-view SEM images of the interfacial microstructure between the SnAg2.5Cu0.8Sb0.5 solder and the Au/Ni(P) metallization after reflow for (a) 1 min, (b) 5 min, (c) 10 min, and (d) 20 min. The solder has been selectively etched away.

A Dage Serious 4000 Bond Tester was used to measure the shear strength of the solder bumps. The test height and speed were 25 μm and 500 μm/s, respectively. Each data point was the average value of 20 bumps from the same die. The microstructure was examined by using a scanning electron microscope (SEM), and energy dispersive spectrum (EDS) was employed to detect the compositions of the intermetallic compounds.

3. Results

3.1. Interfacial reaction

Fig. 2(a–d) displays the cross-sectional SEM images of the SnAg2.5Cu0.8Sb0.5 solder reflowed on the Au/Ni(P) pad metallization for 1, 5, 10, and 20 min, respectively. Both ternary $(Cu,Ni)_6Sn_5$ IMC and Ni_3P layer were observed at the interface. The thickness of the $(Cu,Ni)_6Sn_5$ IMC increased with the increase in reflow time. SEM images of the plan-view of the IMC for the four reflow times are displayed in Fig. 3(a–d). The shape of the $(Cu,Ni)_6Sn_5$ IMC appeared to be rod-type, and its diameter increased with increased reflow time. The composition evolution of the interfacial IMC is listed in Table 1. The Ni content increased from 11.4 to 15.5 at.% as the reflow time increased from 1 min to 20 min, indicating that the Ni in the metallization dissolved into the solders and into the IMC to increase the concentration of the Ni in the $(Cu,Ni)_6Sn_5$ IMC.

Fig. 4(a–d) shows the cross-sectional SEM images of the SnAg3.0Cu0.5Sb0.2 solder reflowed on Au/Ni(P) metallization

Table 1
Compositional evoluation of the $(Cu,Ni)_6Sn_5$ IMC for the SnAg2.5Cu0.8Sb0.5 solder reacted with the Au/Ni(P) metallization pad for different reflow times

Element (at.%)	1 min $(Cu,Ni)_6Sn_5$	5 min $(Cu,Ni)_6Sn_5$	10 min $(Cu,Ni)_6Sn_5$	20 min $(Cu,Ni)_6Sn_5$
Ni	11.4 ± 1.3	14.3 ± 2.4	13.8 ± 0.9	15.5 ± 2.2
Cu	42.3 ± 4.8	44.4 ± 2.9	42.2 ± 0.6	43.8 ± 2.4
Sn	46.3 ± 3.6	41.3 ± 5.0	44.0 ± 0.4	40.7 ± 3.0

Table 2
Compositional evolution of the $(Cu,Ni)_6Sn_5$ and $(Ni,Cu)_3Sn_4$ IMC for the SnAg3.0Cu0.5Sb0.2 solder reacted with the Au/Ni(P) metallization pad for different reflow times

Element (at.%)	1 min		5 min		10 min		20 min	
	$(Cu,Ni)_6Sn_5$	$(Ni,Cu)_3Sn_4$	$(Cu,Ni)_6Sn_5$	$(Ni,Cu)_3Sn_4$	$(Cu,Ni)_6Sn_5$	$(Ni,Cu)_3Sn_4$	$(Cu,Ni)_6Sn_5$	$(Ni,Cu)_3Sn_4$
Ni	18.6 ± 3.3	33.4 ± 2.2	19.2 ± 2.3	32.4 ± 5.9	20.4 ± 1.8	38.6 ± 3.1	19.9 ± 2.4	31.7 ± 2.3
Cu	42.0 ± 6.5	13.1 ± 1.9	40.7 ± 2.5	15.3 ± 3.5	40.7 ± 3.8	11.3 ± 6.7	37.5 ± 6.6	13.3 ± 4.6
Sn	39.4 ± 3.7	53.4 ± 1.6	40.1 ± 0.8	52.3 ± 4.2	38.9 ± 2.0	50.1 ± 8.9	42.6 ± 4.5	55.0 ± 3.2

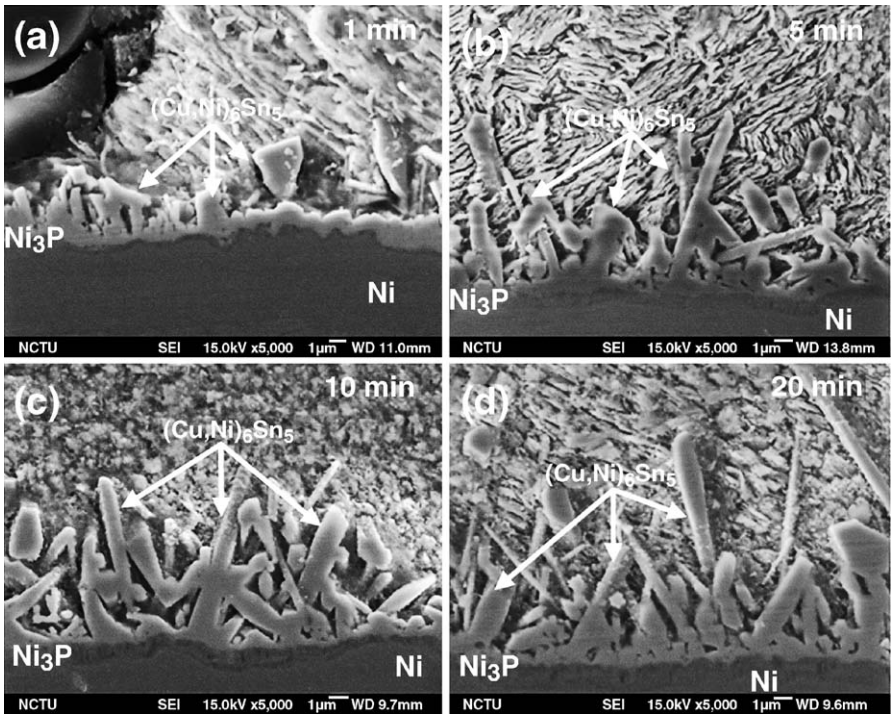

Fig. 4. Cross-sectional SEM images of the interfacial microstructure between the SnAg3.0Cu0.5Sb0.2 solder and the Au/Ni(P) metallization after reflowing for (a) 1 min, (b) 5 min, (c) 10 min, and (d) 20 min.

for 1 min, 5, 10, and 20 min, respectively. The cross-sectional EDS analysis shows that $(Cu,Ni)_6Sn_5$ IMC formed at the interface of the solder and the Ni(P) metallization, and its thickness increased with the reflow time. However, plan-view SEM observations, as shown in Fig. 5(a–d) shows that both $(Cu,Ni)_6Sn_5$ and $(Ni,Cu)_3Sn_4$ IMCs formed at the interface. After reflowing for 1 min, most of the IMC was $(Cu,Ni)_6Sn_5$ IMC. However, its morphology appears to be chunky-type, which is quite different from that in Fig. 3(a). It contains 18.6% of Ni, and the Ni content increased as the reflow time increased, as shown in

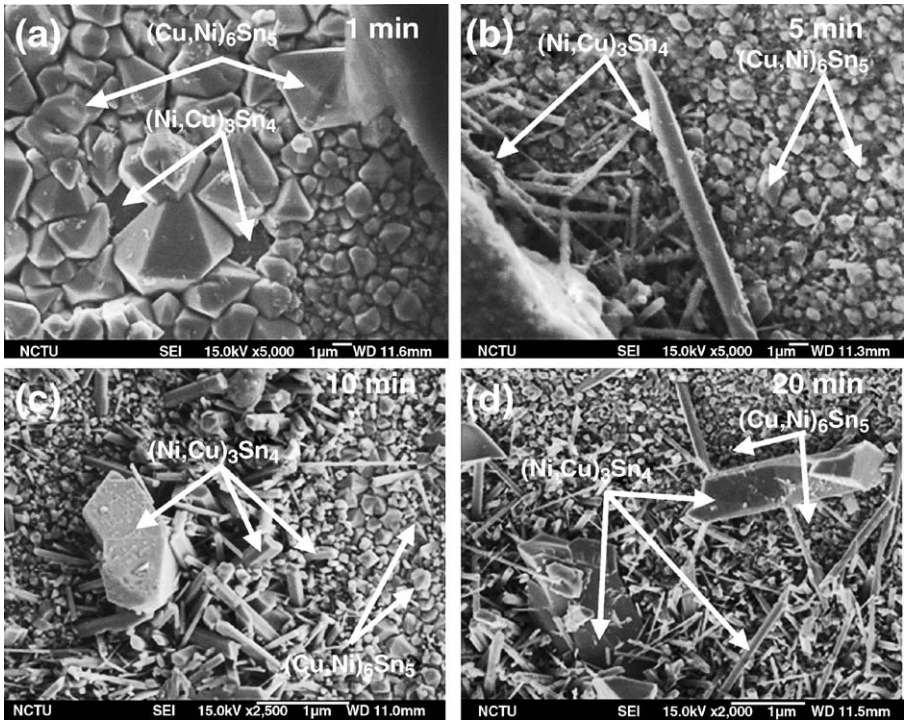

Fig. 5. Plan-view SEM images of the interfacial microstructure between the SnAg3.0Cu0.5Sb0.2 solder and the Au/Ni(P) metallization after reflow for (a) 1 min, (b) 5 min, (c) 10 min, and (d) 20 min. The solder has been selectively etched away. Both $(Cu,Ni)_6Sn_5$ and $(Ni,Cu)_3Sn_4$ IMC formed at the interface.

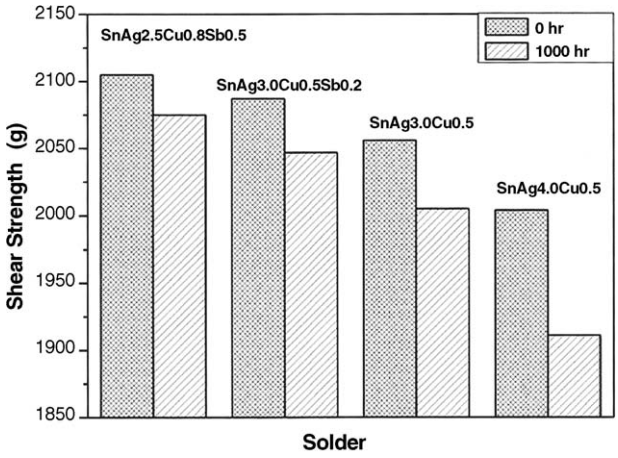

Fig. 6. Shear strength of the four solder bumps before and after the high temperature storage at 150 °C for 1000 h.

Table 2. A small amount of $(Ni,Cu)_3Sn_4$ IMC with 33.4% of Ni was found. As reflow time increased, more $(Ni,Cu)_3Sn_4$ IMC was found, and the shape become rod-like, as indicated by some of the arrows in Fig. 5(a–d).

3.2. Shear strength test

Fig. 6 shows the measured shear strength of the SnAg2.5Cu0.8Sb0.5, SnAg3.0Cu0.5Sb0.2, SnAg3.0Cu0.5, and SnAg4.0Cu0.5 solder bumps both before and after the high temperature storage. It can clearly be seen that the Sb-containing solders have higher shear strength than the SnAgCu solders. As the amount of Sb addition increased, the shear strength increased slightly. In addition, shear strength for the four solder bumps decreased after high temperature storage, which may be due to the coarsening of the Ag_3Sn IMC and grain growth of the solder. Fig. 7(a and b) shows the cross-sectional (BSE) SEM images of the SnAg2.5Cu0.8Sb0.5 solder bumps before and after the high temperature storage, respectively. The coarsening of the $(Cu,Ni)_6Sn_5$ IMC can be clearly observed in Fig. 7(b) after the high temperature storage. Fig. 7(c and d) reveals the fracture surfaces for the SnAg2.5Cu0.8Sb0.5 solder bumps before and after the high temperature storage, respectively. It can be seen that the fractures occurred inside the solder bumps. Fig. 8(a and b) shows the cross-sectional (BSE) SEM images of the SnAg3.0Cu0.5Sb0.2 solder bumps before and after the high temperature storage, respectively. Plate-like Ag_3Sn IMC can be clearly observed inside the solder after the high temperature storage. Fig. 8(c and d) shows the fracture surfaces for the SnAg3.0Cu0.5Sb0.2 solder bumps before and after the high temperature storage, respectively. Similar to the SnAg2.5Cu0.8Sb0.5 solder bumps, the fractures occurred inside the solder bumps. For SnAg3.0Cu0.5 and SnAg4.0Cu0.5 solder bumps, the fractures were also found inside the solder bumps.

4. Discussion

The difference in IMC formation for the two solders may be attributed to the Cu concentration in the solders. Chen et al. investigated the effect of Cu addition on the reaction between Sn and Ni, finding that when the Cu concentration was between 0.4 and 0.6%, both $(Ni,Cu)_3Sn_4$ and $(Cu,Ni)_6Sn_5$ IMCs formed

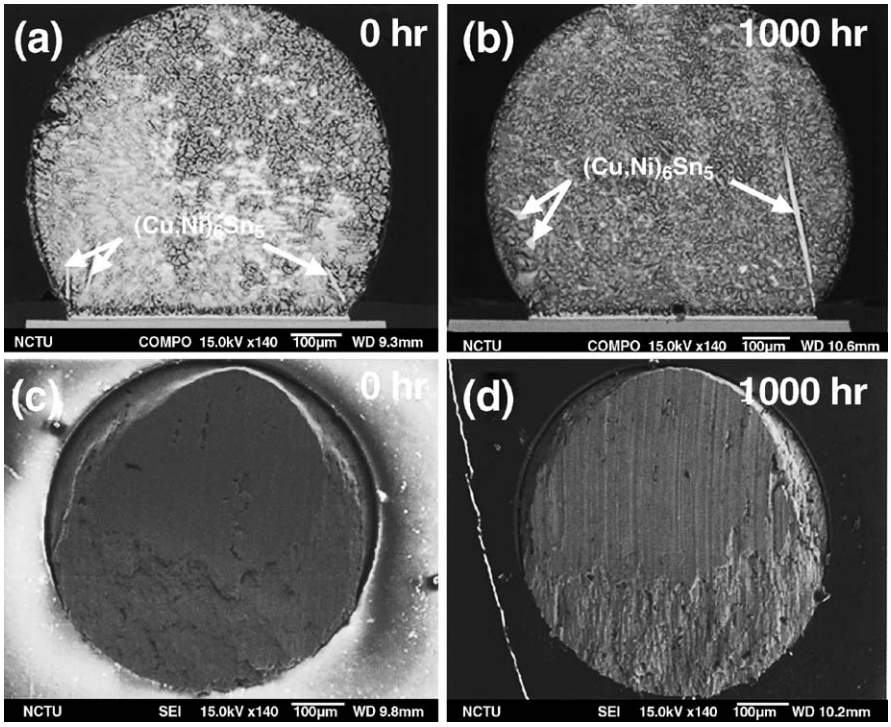

Fig. 7. (a) Cross-sectional SEM image of the SnAg2.5Cu0.8Sb0.5 solder bump on Au/Ni(P) metallization before the high temperature storage; and (b) after high temperature storage at 150 °C for 1000 h. Fracture surface of the SnAg2.5Cu0.8Sb0.5 solder bump (c) before the high temperature storage; and (d) after high temperature storage at 150 °C for 1000 h.

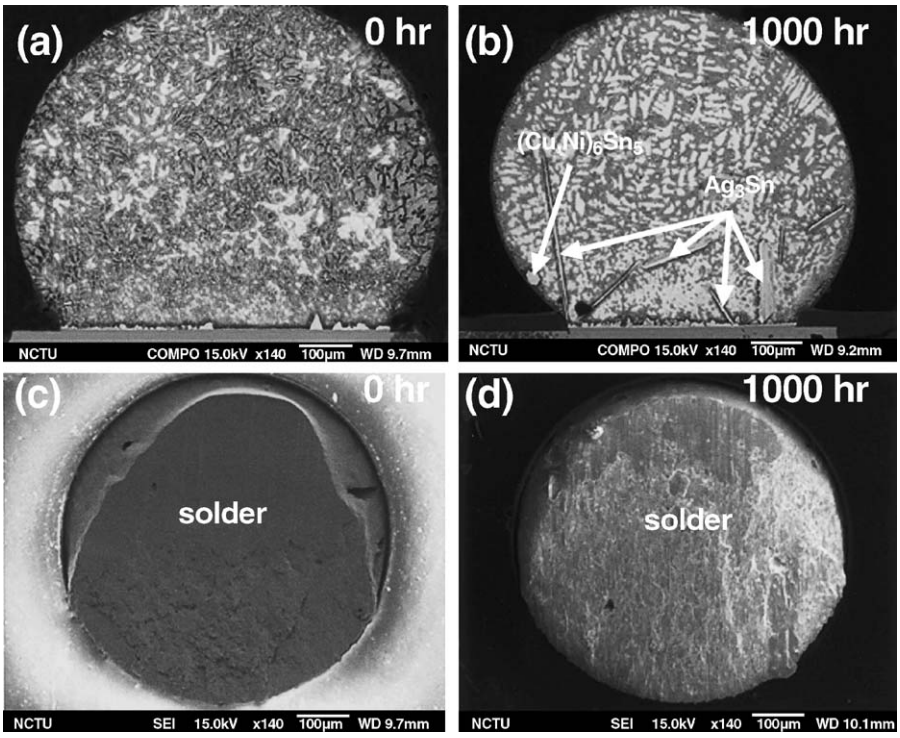

Fig. 8. (a) Cross-sectional SEM image of the SnAg3.0Cu0.5Sb0.2 solder bump on Au/Ni(P) metallization layer before the high temperature storage; and (b) after the high temperature storage at 150 °C for 1000 h. Fracture surface of the SnAg3.0Cu0.5Sb0.2 solder bump (c) before the high temperature storage; and (d) after the high temperature storage at 150 °C for 1000 h.

[10]. However, when the Cu concentration was higher than 0.6%, the only stable IMC was $(Cu,Ni)_6Sn_5$. In our study, both $(Cu,Ni)_6Sn_5$ and $(Ni,Cu)_3Sn_4$ IMCs formed when the Cu concentration was 0.5 wt% for the SnAg3.0Cu0.5Sb0.2 solder, and only $(Cu,Ni)_6Sn_5$ IMC was found when the Cu concentration was 0.8 wt% for the SnAg2.5Cu0.8Sb0.5 solder. These results agree with theirs. Therefore, the reason for the difference in the IMC formation between the two solders is mainly due to the difference in the Cu content in the solders, and it may be independent of the Sb concentration in the solders.

The results of shear strengths indicate that the addition of Sb could strengthen the β-Sn solder matrix. Furthermore, as the amount of Sb addition increased, the shear strength increased slightly. Lee et al. reported that some Sb atoms may dissolve into the β-Sn matrix to strengthen the solder, and some of them may exist in the form of ε-$Ag_3(Sb,Sn)$ IMC when the addition of Sb is less than 1.75% [15]. The later may not be able to strengthen the SnAgCu solder, since the Sb atom substitutes for the Sn atoms. In addition, Lee et al. investigated the adhesive strength of Cu/SnAg/Cu by adding various concentration of Sb into SnAg solder, finding that the adhesive strength of SnAg solders increased with the Sb addition [9]. Nevertheless, 1.5% Sb addition shows a higher adhesive strength than 2% Sb addition in SnAg solder joints. In our research, we investigated the effect of 0.2 and 0.5% Sb addition on the shear strength in SnAgCu solder bumps. The results also revealed that SnAg2.5Cu0.8Sb0.5 solder had higher shear strength than SnAg3.0Cu0.5Sb0.2, which agreed with the previous results. Since the fracture occurred inside the solder, the difference in shear strength should be independent of the interfacial IMC. Furthermore, for SnAg3.0Cu0.5Sb0.2 and SnAg3.0Cu0.5 solder, the only difference is the addition of 0.2% Sb, and the shear strength of the SnAg3.0Cu0.5Sb0.2 solder has slightly higher shear strength than the SnAg3.0Cu0.5 solder. Therefore, it can be inferred that the difference in Sb concentration causes the difference in the shear strength.

SnAg4.0Cu0.5 has the lowest shear strength in samples both with and without high temperature storage. Several studies have reported that the large plate-like Ag_3Sn structures can grow rapidly within the liquid phase during cooling and could adversely effects the mechanical property of solder joints [1,11–14]. It is speculated that higher concentration of Ag in the solder may form more and large plate-like Ag_3Sn compounds in the solder. If Ag_3Sn compounds form in a region of stress concentration, cracks will be easily initiated and thus propagate in the solder bumps. Therefore, SnAg4.0Cu0.5 solder has the lowest shear strength compared with SnAg2.5Cu0.8Sb0.5, SnAg3.0Cu0.5Sb0.2, and SnAg3.0Cu0.5 solders.

5. Conclusions

We have studied the metallurgical reactions and shear strength of the two commercial Sb-containing solders with the Au/Ni(P) metallization layer. It is found that only $(Cu,Ni)_6Sn_5$ IMC formed in SnAg2.5Cu0.8Sb0.5 solder and both $(Cu,Ni)_6Sn_5$ and $(Ni,Cu)_3Sn_4$ IMCs formed in SnAg3.0Cu0.5Sb0.2 solder. In addition, the addition of Sb in the SnAgCu solder increased the shear strength of the solder. The

SnAg2.5Cu0.8Sb0.5 solder has higher shear strength than the SnAg3.0Cu0.5Sb0.2, SnAg3.0Cu0.5, and SnAg4.0Cu0.5 solders.

Acknowledgement

The authors would like to acknowledge the financial support of the National Science Council of Taiwan through Grant No. NSC92-2216-E009-008.

References

[1] K.N. Tu, A.M. Gusak, M. Li, J. Appl. Phys. 93 (2003) 1335.
[2] D. Suraski, K. Seelig, IEEE Trans Electron. Pack. Manufact. 24 (4) (2001) 244.
[3] See website http://www.nemi.org/PbFreePUBLIC.
[4] K. Zeng, K.N. Tu, Mater. Sci. Eng. Rep. R38 (2002) 55.
[5] T.Y. Lee, W.J. Choi, K.N. Tu, J.W. Jiang, S.M. Kuo, J.K. Lin, J. Mater. Res. 17 (2002) 291.
[6] M. Amagai, Y. Toyoda, T. Tajima, in: Proceedings of the 53th Electronic Component and Technology Conference, New Orleans, LA, 2003, p. 317.
[7] X. Ma, R. Wang, Y. Qian, F. Yoshida, Mater. Lett. 57 (2003) 3361.
[8] B.L. Chen, G.Y. Li, Thin solid film 462–463 (2004) 395.
[9] H.T. Lee, M.H. Chen, H.M. Jao, C.J. Hsu, J. Electron. Mater. 33 (9) (2004) 10448.
[10] W.T. Chen, C.E. Ho, C.R. Kao, J. Mater. Res. 17 (2) (2002) 263.
[11] S.K. Kang, D.Y. Shih, D. Leonard, D.W. Herderson, T. Gosseline, S. Cho, J. Yu, W.K. Choi, JOM 56 (6) (2004) 34.
[12] D.R. Frear, J.W. Jang, J.K. Lin, C. Zang, JOM 53 (6) (2001) 28.
[13] K.S. Kim, S.H. Huh, K. Suganuma, Mater. Sci. Eng. A333 (2002) 106.
[14] D.W. Henderson, T. Gosselin, A. Sarkhel, S.K. Kang, W.K. Choi, D.Y. Shih, C. Coldsmith, K.J. Puttlitz, J. Mater. Res. 17 (11) (2002) 2775.
[15] H.T. Lee, T.L. Liao, M.H. Chen, The 3rd International Symposium on Electronics and Packaging, Jeju Island, Korea, 2001, p. 315.